

Fig. 2. Type of link models: (a) communication link from MCRBS to MCRBS, (b) communication link from MCRBS to user, (c) communication link from user to MCRBS, and (d) communication link from user to user.

or resource scheduling mechanism, the inter-cell interference can be managed efficiently. Therefore, we place an emphasis on the intra-cell interference, which is due to resource sharing of D2D and cellular communication.

In disaster effected areas, if the cellular base stations are still remain, recovery network provisioning can be extended by using device to device (D2D) approaches such as in reference [9] [10] which proposes an innovative resource allocation scheme by introducing the device freedom to multiplex multiple D2D and cellular users for increasing the spectrum efficiency. In contrast, when there is no infrastructure operating, MCRBS should be a more practical option. However, the previous works related to MCRBS mainly focus on possible routes number to determine number of nodes.

In this paper, we focus on possible routes number to know the number of nodes that is used for routing of MCRBS for DRN. When possible routes number are known, it is possible to determine number of nodes.

The rest of the paper is organized as follows. Section II introduces our system model. Section III introduces proposed technologies. The performance evaluation presented in Section IV. Finally, Section V concludes the paper.

II. SYSTEM MODEL

In this paper, we consider link connection by nodes, where the nodes are MCRBS and device used by victim or user. When disaster occurs, transmitter and receiver need nodes to

create connection. Routing is set of links which is connected to each other. Fig. 2 shows four types of link that are used in this paper. Modulation, coding, and synchronization assume perfect in system model. This model used Rayleigh fading channel.

This paper uses frequency-flat Rayleigh fading with distribution function from received signal normalization that change by time [11]. Probability density function (PDF) from Rayleigh fading is

$$p(\tau) = \frac{r}{\sigma^2} \exp\left(-\frac{r^2}{2\sigma^2}\right), \quad (1)$$

where σ is value of root mean square (rms) from received signal, σ^2 is the variance of the received signal, and $\frac{r^2}{2}$ is received power. Rayleigh fading channel in this paper can be expressed as

$$\mathbf{y} = h \cdot \mathbf{c} + \mathbf{n}, \quad (2)$$

where c is the number of bit sent, n is noise vector and h is variable random complex. We obtained h for frequency-flat Rayleigh fading channel based on MATLAB simulation with $h_f = (\text{rand} + \sqrt{-1} \cdot \text{randn})/\sqrt{2}$.

In reference [12] the dynamic of fading channels are exploited to improve the decoding success probability due to the diversity effect. The idea of exploiting dynamic fading channels is from the fact that a link is dropped or assumed to be erased when the received power is below a threshold T_h , of which the probability is

$$\begin{aligned} Pr(\gamma \leq Th) &= \int_0^{Th} Pr(\gamma) d\gamma \\ &= 1 - e^{-\frac{Th}{\Gamma}}, \end{aligned} \quad (3)$$

where $Pr(\gamma) = \frac{1}{\Gamma} \exp(-\frac{\gamma}{\Gamma})$ [13]. Without loss of generality, we assume that $\Gamma = 1$ for simplicity, and T_h of 10^{-10} , 10^{-9} , and 10^{-8} .

Radio propagation model COST 231 Walfisch-Ikegami is extension from COST Hata model [14]. This model range of validity carrier frequency f_c 800 until 2000 MHz. The COST-231 model is a pathloss model for the case of small distance between mobile station (MS) and base station (BS), and/or small height of the MS. The pathloss total for the *line of sight* (LOS) case is given by

$$P_l = 42.6 + 26 \log_{10}(d) + 20 \log_{10}(f_c) \quad (4)$$

for $d \geq 20m$ with range of validity 0.02 until 5 kilometer, where again d is in units of kilometers, and f_c is in units of MHz [15].

III. POSSIBLE ROUTING

Algorithm 1 provides a routing method for possible routes number of nodes. In this paper we simulate three cases based on location and battery lifetime condition

- 1) Uniform location and uniformly full battery lifetime.
- 2) Random location and uniformly full battery lifetime.

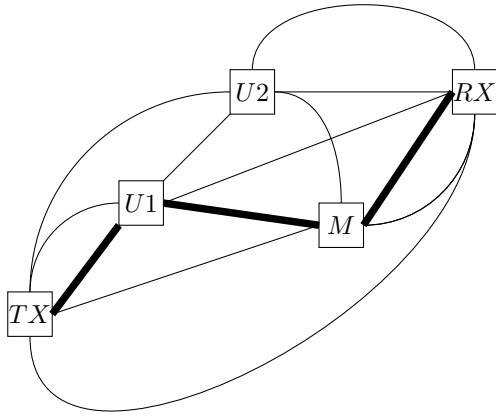


Fig. 3. An illustration of a routing utilizing three nodes U_1, U_2 and M .

TABLE I
REPRESENTATION OF ROUTES CONNECTED BY LINKS IN FIG. 3.

Node	TX	U1	M	U2	RX
TX	0	1	1	1	1
U1	0	0	1	1	1
M	0	0	0	1	1
U2	0	0	0	0	1
RX	0	0	0	0	0

- 3) Random location and random battery lifetime ($B \geq 30\%$, $B \geq 50\%$, and $B \geq 70\%$).

We consider to simulate random location and random battery lifetime because this condition will real happened when DRN occur. We also consider to set threshold of battery lifetime for each node. If battery lifetime of node less than threshold, then node will not be connected and routed.

Fig. 3 shows the illustration of routing using three nodes from transmitter to receiver. TX is transmitter, RX is receiver, node (U_1, U_2) are device of victims and node M is MCRBS. The formula to maximal possible number of route is 2^N , where N is number nodes. For example, for three nodes (2^3), we will get the maximum number of route is eight. Table I show

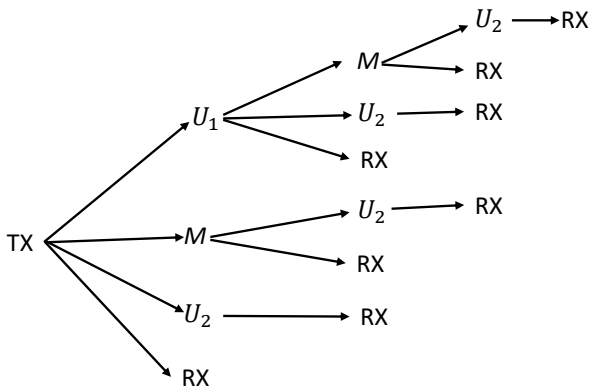


Fig. 4. Representation of links connecting as routes in Table I.

TABLE II
SIMULATION SETTINGS

Parameters	Value
Circle radius area disaster	2.5 km
Number of node (N)	1 - 10
Threshold power (T_h)	10^{-10} , 10^{-9} , and 10^{-8}
Threshold BER	10^{-4} , 10^{-3} , and 10^{-2}
Pathloss exponent (n)	2.6

representative value of links from Fig. 3, i.e., route of links are $TX-U_1-M-RX$.

Fig. 4 demonstrates of links connection to get routes from value of Table I. The first route is $TX-U_1-M-U_2-RX$, the second route is $TX-U_1-M-RX$, the third route is $TX-U_1-U_2-RX$, the fourth route is $TX-U_1-RX$, the fifth route is $TX-M-U_2-RX$, route the sixth route is $TX-M-RX$, the seventh route is $TX-U_2-RX$, and the eighth route is $TX-RX$.

IV. PERFORMANCES EVALUATION

In order to validate the analytical findings and evaluate the performance of our proposed algorithm, we conduct extensive computer-based simulation. In this section, we present the settings of the simulations and the performance evaluation results.

A. Simulation Settings

The simulation settings are summarized in Table I where we can see area have circle radius area disaster 2.5 km, 1-10 nodes, and threshold power of 10^{-10} , 10^{-9} , and 10^{-8} , threshold BER of 10^{-4} , 10^{-3} , and 10^{-2} , and pathloss exponent of 2.6 refer to (4). Affected by location, there are uniform and random, link power, and battery (B) lifetime, which consist of uniformly full (we assume of 100%) and random (we assume of threshold battery are $B \geq 30\%$, $B \geq 50\%$, and $B \geq 70\%$).

B. Routing Base on Signal Stregh

1) *Uniform Location and Uniformly Full Battery Lifetime:* Fig. 5 demonstrates the relationship between possible number of routes and nodes with location uniform and uniformly full battery lifetime. X axis is number of nodes (N) and Y is axis possible routes number. Location uniform means nodes position are arranged and uniformly full battery lifetime means nodes battery lifetime 100%. The solid line curve is for possible route number with one MCRBS and the dashed line curve is for possible route number without MCRBS. Fig. 5 shows that the more nodes then the more possible number of routes.

2) *Random Location and Uniformly Full Battery Lifetime:* Fig. 6 demonstrates the relationship between possible number of routes and nodes with random location and uniformly full battery lifetime. X axis is number of nodes (N) and Y is axis possible routes number. Random location means nodes position is random, and uniformly full battery lifetime means meaning nodes battery lifetime is 100%. The solid line curve is for possible route number with one MCRBS and the dashed

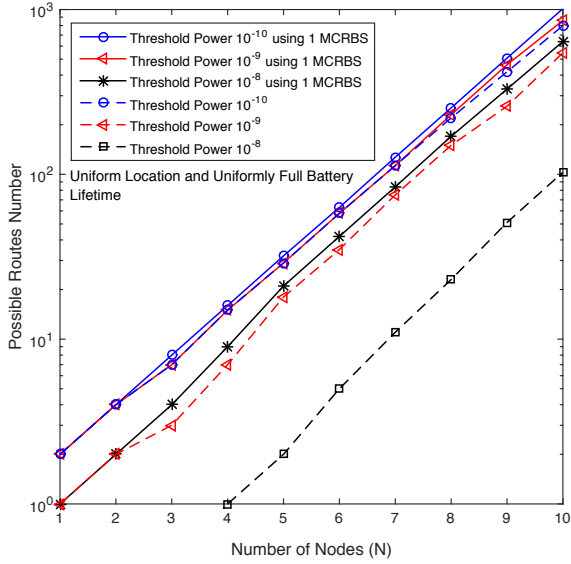


Fig. 5. The number of possible routes simulated in disaster area, where the helping nodes are distributed uniformly with uniform remaining battery lifetime.

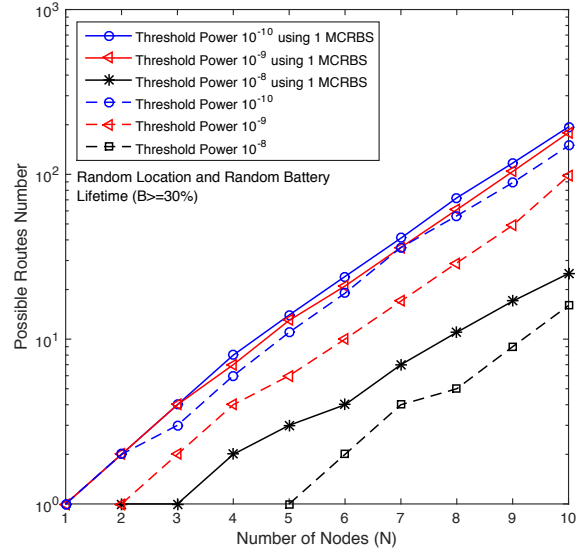


Fig. 7. The number of possible routes simulated in disaster area, where the helping nodes are distributed randomly as well as the random remaining battery lifetime beyond 30%.

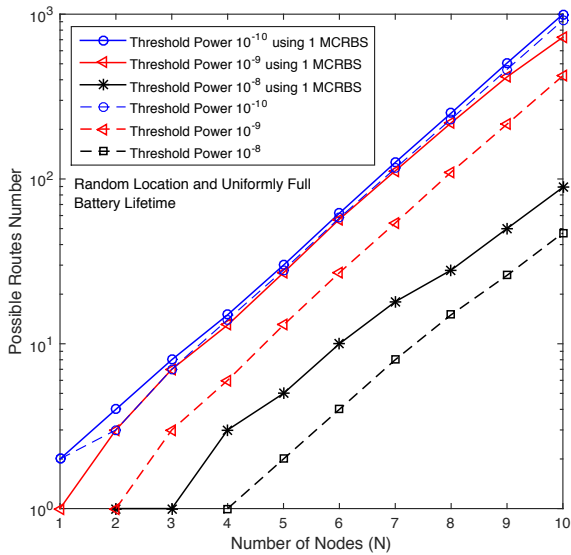


Fig. 6. The number of possible routes simulated in disaster area, where the helping nodes are distributed randomly and fix remaining battery lifetime.

line curve is for possible route number without MCRBS. Possible routes number decrease because it is influenced by random location.

3) *Random Location and Random Battery Lifetime*: This experiment assume as use battery lifetime random of $B \geq 30\%$, $B \geq 50\%$, and $B \geq 70\%$. X axis is number of nodes (N) and Y is axis possible routes number. The solid line curve is for possible route number with one MCRBS and the dashed

line curve is for possible route number without MCRBS. This simulation adjusted according to real disaster situation. For Fig. 7 demonstrates the random location and battery lifetime random with battery $B \geq 30\%$, Fig. 8 demonstrates the random location and battery lifetime random with battery $B \geq 50\%$, and Fig. 9 demonstrates the random location and battery lifetime random with battery $B \geq 70\%$. Battery influence possible routes number, if battery lifetime is lower, then possible routes number automatically become lesser.

C. Routing Based on Reliability

In this subsection, we measure the possible routes using the link reliability measured theoretically based on

$$\text{BER}_{\text{fading}} = 0.5 \cdot \left(1 - \frac{1}{\sqrt{1 + \frac{1}{\gamma}}} \right), \quad (5)$$

where γ is the signal to noise power ratio (SNR) for the corresponding link. We assume 1 until 10 nodes, noise power of -109 dBm, and -90 dBm, and power transmitter P_{tx} 20 dB. We simulate to use threshold BER of 10^{-4} , 10^{-3} and 10^{-2} as the minimum SNR to construct a route. These values are selected in this paper, because all evaluated communication links are without channel coding. With channel coding, the quality is improved.

Since BER in (5) requires SNR γ for the given link, we consider a receive SNR of the link expressed as

$$\gamma = ((P_{tx}/P_l) * |h_f|^2 * G)/N, \quad (6)$$

where P_{tx} is power transmitter, P_l is pathloss, $n = 2.6$ is pathloss exponent, h_f is fading, G is gain, N is noise, and

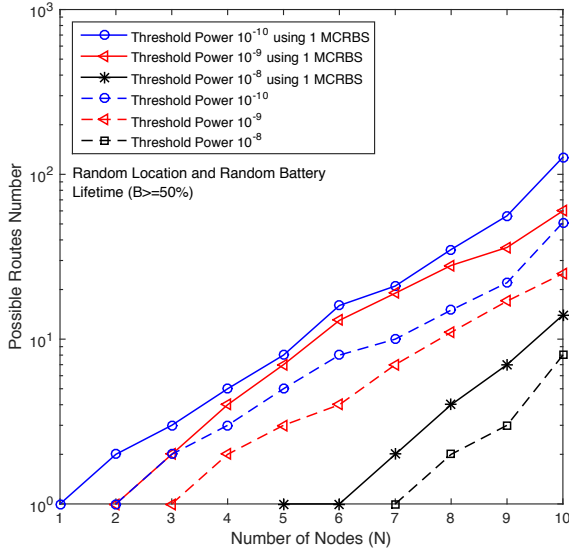


Fig. 8. The number of possible routes simulated in disaster area, where the helping nodes are distributed randomly as well as the random remaining battery lifetime beyond 50%.

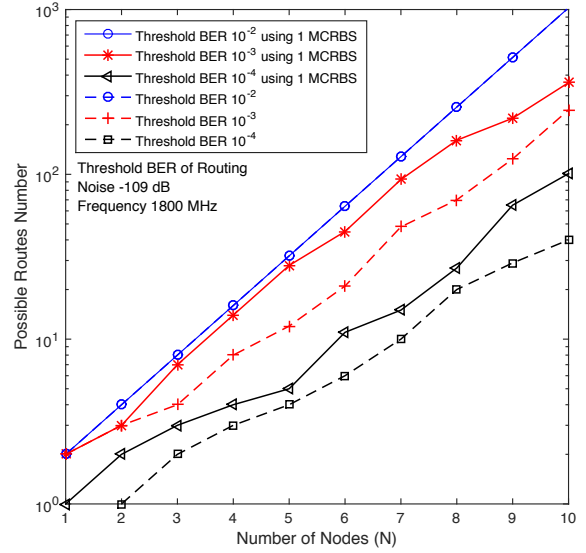


Fig. 10. The number of possible routes simulated in disaster area, where the helping nodes are distributed randomly with P_{tx} 20 dB and using noise -109 dBm.

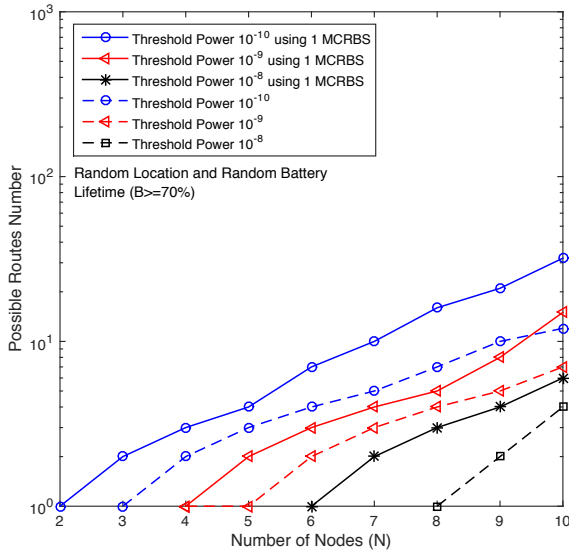


Fig. 9. The number of possible routes simulated in disaster area, where the helping nodes are distributed randomly as well as the random remaining battery lifetime beyond 70%.

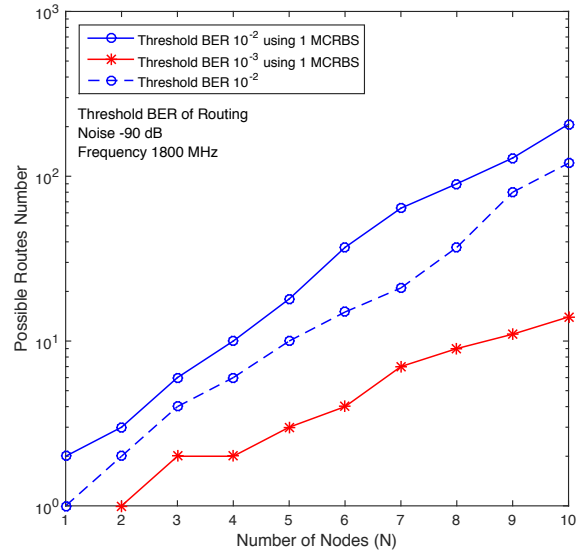


Fig. 11. The number of possible routes simulated in disaster area, where the helping nodes are distributed randomly with P_{tx} 20 dB and using noise -90 dBm.

P_{tx} is the transmit power of each link in the considered route. P_{tx} may vary according to the remaining battery lifetime.

1) *Random Location and Random Battery Lifetime*: This experiment assume as use random location and battery lifetime random using threshold battery lifetime of $B \geq 30\%$, and this simulation used one MCRBS with the power of 30 dB for every simulations node number. Fig. 10 demonstrates possible routes number using noise -109 dBm and Fig. 11 demonstrates

possible routes number using noise -90 dBm. The solid line curve is for possible route number with one MCRBS and the dashed line curve is for possible route number without MCRBS. As shown in the Figs. 10 and 11, network with one MCRBS has higher possible route number, and 10th node has more possible route than the other smaller node. Moreover the number of possible route are slightly affected by the power transmitter.

V. CONCLUSION

In this paper, we have proposed a wireless DRN based on routing algorithm using MCRBS, where optimal routes are constructed by considering the remaining battery lifetime and number of helping nodes, either victims devices or MCRBS. We have used three parameters for constructing the routes, i.e., threshold power, remaining battery lifetime, and link quality. The proposed DRN has constructed many possible routes based on the number of available helping nodes, where we found that the MCRBS helps to increase the number of possible routes for successful communications to the normal region. These results are expected to help the development of future routing algorithm for DRN utilizing the available active devices in the area suffering from disaster.

REFERENCES

- [1] J. Xu, K. Ota, and M. Dong, "Fast networking for disaster recovery," *IEEE Transactions on Emerging Topics in Computing*, pp. 1–1, 2017.
- [2] T. Ngo, H. Nishiyama, N. Kato, S. Kotabe, and H. Tohjo, "A novel graph-based topology control cooperative algorithm for maximizing throughput of disaster recovery networks," in *2016 IEEE 83rd Vehicular Technology Conference (VTC Spring)*, May 2016, pp. 1–5.
- [3] A. Nosratinia, T. E. Hunter, and A. Hedayat, "Cooperative communication in wireless networks," *IEEE Communications Magazine*, vol. 42, no. 10, pp. 74–80, October 2004.
- [4] S. Yang, Z. Sheng, J. A. McCann, and K. K. Leung, "Distributed stochastic cross-layer optimization for multi-hop wireless networks with cooperative communications," *IEEE Transactions on Mobile Computing*, vol. 13, no. 10, pp. 2269–2282, October 2014.
- [5] Z. Mo, W. Su, S. Batalama, and J. D. Matyjas, "Cooperative communication protocol designs based on optimum power and time allocation," *IEEE Transactions on Wireless Communications*, vol. 13, no. 8, pp. 4283–4296, August 2014.
- [6] T. Kobayashi, S. Seimiya, K. Harada, M. Noi, Z. Barker, G. K. Woodward, A. Willig, and R. Kohno, "Wireless technologies to assist search and localization of victims of wide-scale natural disasters by unmanned aerial vehicles," in *2017 20th International Symposium on Wireless Personal Multimedia Communications (WPMC)*, December 2017, pp. 404–410.
- [7] S. Xu, H. Wang, T. Chen, Q. Huang, and T. Peng, "Effective interference cancellation scheme for device-to-device communication underlying cellular networks," in *2010 IEEE 72nd Vehicular Technology Conference - Fall*, September 2010, pp. 1–5.
- [8] C. H. Yu, K. Doppler, C. B. Ribeiro, and O. Tirkkonen, "Resource sharing optimization for device-to-device communication underlying cellular networks," *IEEE Transactions on Wireless Communications*, vol. 10, no. 8, pp. 2752–2763, August 2011.
- [9] C. Xu, L. Song, Z. Han, Q. Zhao, X. Wang, X. Cheng, and B. Jiao, "Efficiency resource allocation for device-to-device underlay communication systems: A reverse iterative combinatorial auction based approach," *IEEE Journal on Selected Areas in Communications*, vol. 31, no. 9, pp. 348–358, September 2013.
- [10] B. Narottama, A. Fahmi, R. P. Astuti, D. M. Saputri, N. Andini, H. Vidyanyingtyas, P. E. Christy, O. R. Ludwiniananda, and F. Rachmawati, "Base station energy efficiency of D2D device discovery," in *2017 International Conference on Control, Automation and Information Sciences (ICCAIS)*, October 2017, pp. 257–261.
- [11] V. Garg, *Wireless Communications and Networking*. Elsevier, 2007.
- [12] K. Anwar, "Graph-based decoding for high-dense vehicular multiway multirelay networks," in *2016 IEEE 83rd Vehicular Technology Conference (VTC Spring)*, May 2016, pp. 1–5.
- [13] K. Anwar, Juansyah, B. Syihabuddin, and N. M. Adriansyah, "Coded random access with simple header detection for finite length wireless IoT networks," in *2017 Eighth International Workshop on Signal Design and Its Applications in Communications (IWSDA)*, September 2017, pp. 94–98.
- [14] C. A. 231, *Digital mobile radio towards future generation systems, final report*. European Communities, EUR 18957, 1999.
- [15] *Wireless Communications, Second Edition*. John Wiley, 2011.

Algorithm 1 Possible Routes Construction

1. Matrix $S = a$
4. **FOR** $i=1:\text{length}(S)$
5. **FOR** $j=1:\text{length}(S)$
6. **IF** value element $S = 1$
7. Save value node and relation [$i j$]
8. **END IF**
9. **END FOR**
10. **END FOR**
11. **IF** matrix store no EMPTY
12. Initialization $\text{startNode} = \text{store}(1,1)$
13. Initialization cell matrix $\text{startNodeArr} = \{\}$
14. Initialization matrix $\text{childNode} = []$;
15. **FOR** $i=1:\text{length}(\text{store}(:,1))$
16. **IF** $(\text{store}(i,1) == \text{startNode})$
17. Save/add value $\text{store}(:,1)$ to matrix startNodeArr
18. **ELSE**
19. Save/add value $\text{store}(:,1)$ to matrix childNode
20. **END IF**
21. **END FOR**
22. Initialization cell matrix $\text{currentRoutes} = \{\}$
23. $\text{findLastNodeAll} = 0$
24. **FOR** $mm=1:\text{length}(\text{startNodeArr})$
25. **IF** the last value from element cell startNodeArr equal to the last node (the first node directly go to the last node)
26. Save/add ke matrix allRoutes
27. **END IF**
28. **END FOR**
29. **IF** $(\text{length}(\text{startNodeArr}) == 1)$
30. $\text{findLastNodeAll} = 1$ (there is only one route)
31. **END IF**
32. **WHILE** $(\text{findLastNodeAll} == 0)$
33. Initialization cell matrix $\text{currentRoutes} = \{\}$
35. $\text{startNodeArr} = \text{currentRoutes}$
36. $\text{complete} = 1$;
37. $ii = 1$;
38. **WHILE** $\text{complete} \ \&\& \ ii=\text{length}(\text{currentRoutes})$
39. Save value index element where $\text{currentRoutes}ii,1 == \text{length}(S)$ to have variable
40. **IF** $\text{have} == 0$
41. $\text{complete} = 0$;
42. **END IF**
43. $ii = ii+1$
44. **END WHILE**
45. **IF** $(\text{complete} == 1)$
46. $\text{findLastNodeAll} = 1$;
47. **END IF**
48. **END WHILE**
49. **END IF**
